ICSV14
Cairns • Australia
9-12 July, 2007
14th International Congress on Sound & Vibration

STEPWISE AIR FLOW IN THE GRAVITY DRAUGHT AEROACOUSTIC TUNNEL

Radu Dan Rugescu[1]

[1] Department of Aerospace Engineering, Texas A&M University
701 H. R. Bright Building, Ross St, 3141 TAMU, College Station, TX 77843, USA
rugescu@yahoo.com, rugescu@aero.tamu.edu

Abstract

Numerical simulation of non-isentropic and discontinuous unsteady flows with energy addition or extraction, during ignition of solid propellant rocket motors was modified to simulate transients of the airflow in tall solar towers based on the wave front method. Zannetti previously used this method for isentropic flows in high-speed aerodynamics. Its application in discontinuous flows through equation change and local energy extraction also proves highly efficient. Computational efficiency is demonstrated by CFD simulation of the starting transients in solar towers and the WINNDER aeroacoustic wind tunnel in particular. The 1-D methodology and numerical code are especially suited for unsteady flows in slender channels, where the ratio between the length of the duct and its diameter is high. The wave front model scheme covers the dual behaviour of the fully non-isentropic flow in the heat exchanger and the isentropic flow through the test chamber. Code robustness is demonstrated during runs on the PC. The 1-D numerical scheme is based on resolution of gasdynamic discontinuities within the enhanced method already proven for solid propellant rocket motors.

Keywords: unsteady methods, solar gravity draught, aeroacoustics, wind tunnel

1. PRESENT STATUS IN UNSTEADY FLOW COMPUTER CODES

Successful in describing continuous flows of normal air in aerodynamics, the wave front method [1] was first extended [3], [4] to the wholly non-isentropic flows with sharp discontinuities in solid rocket engines (SRE). The applicability of the extended wave front method to unsteady flows in the SEATTLER solar mirror gravity-assisted (SMG), tall tower wind tunnel [4], [5], [6], [7] is now at the beginning of a full demonstration.

A different concept as compared to SEATTLER was built so far as the only existing experimental power plant located near the Manzanares River in Spain [8]. The innovative modification of this technology of the gravitational draught as described below was already modelled by the 0-D method, during a previous CNCSIS grant in Romania. There are known some approaches by the 0-D model [9] to demonstrate the feasibility of the Solar Tower concept, all focused on the greenhouse system. In contrast to the greenhouse heater, the solar mirror concentrator is by far more efficient [10].

The combination of the mirror with the draught tower [4] is a major improvement. The Zannetti 1-D approach by the wave front model was first extended to SRE-s [2]. The 1-D approach is well justified in solar mirror gravity draught due to the slender aspect of the channels in the tower. The *Transit* unsteady code is a very applied tool for studying the instabilities revealed by the present 0-D model of WINNDER. A simple physical model is first considered. In case of MGT, the short zone of heating at the tower base is continued with the adiabatic gravity draught within the tall tower (Fig. 1). The jump in the internal flow is resolved in the 1-D treatment that follows, physically motivated for all slender configurations like SRE-s and tall solar towers as well.

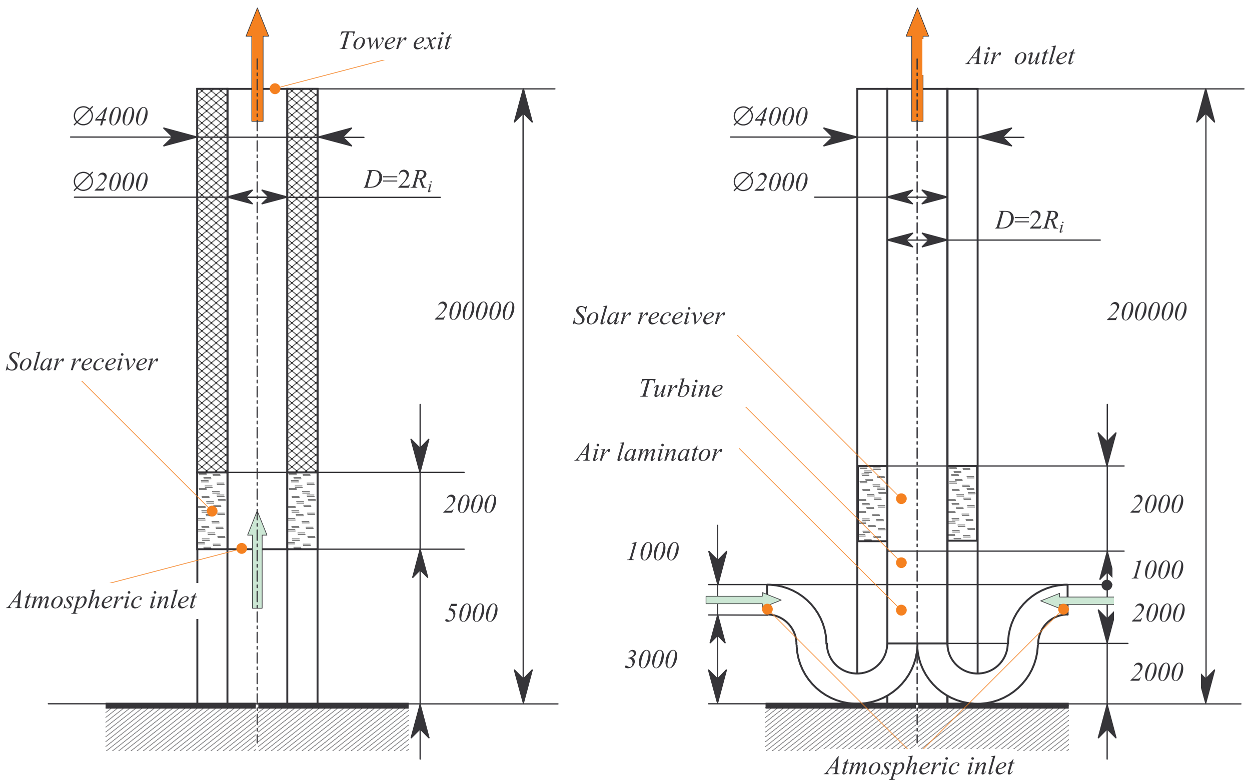

Figure 2: Schematic draft of the WINNDER/SEATTLER solar-mirror gravity-draught rigs.

While the diameter of the receiver equals 1 meter and its height equals the height of all the individual mirrors of the array, the maximal amplification of the natural insolation of regularly 1 W/m^2 is proportional to the squared mirror array external radius. Consequently $q=R_e^2/4\ W/m^2$. For a 200 m array it results $q=10\ kW/m^2$.

2. UNSTEADY FLOWS THROUGH THE ONE-DIMENSIONAL WAVE FRONT METHOD OF ZANNETTI.

In order reduce the phenomenon to a simple longitudinal overall motion of the working fluid, an insight to the process must proceed. The assumed hypotheses are the following [7]:

1. The inlet is planar where the air is accelerated along a compressible or incompressible Bernoulli law upon request;
2. The heating zone receives an ever-*constant* heat flux q and given friction law;
3. The gravity draught zone performs adiabatic, namely with no heat exchange with the surroundings;
4. The intensity of gravity is strongly constant due to the negligible height of the tower;
5. The polytropic atmosphere is considered to model the gravity draught;

6. At the upper exit from the tower the local static pressure from inside and outside balance at equal levels;
7. A uniform distribution of parameters within every cross-area of the tower subsists.

These presumptions have a simplifying, some of them apparently conflicting, but all of them an indispensable character. To cover the MGT case these equations are completed with the effect of heat transfer, friction and the gravitational draught:

$$\frac{\mathrm{D}}{\mathrm{D}t}\int_{\mathrm{d}\upsilon}\rho\,\mathrm{d}\upsilon = \frac{\partial}{\partial t}\int_{\mathrm{d}\upsilon}\rho\,\mathrm{d}\upsilon + \int_{\partial\upsilon}\rho v_n\,\mathrm{d}s = 0\,, \tag{1}$$

$$\frac{\mathrm{D}\mathbf{H}}{\mathrm{D}t} = \frac{\partial}{\partial t}\int_{\mathrm{d}\upsilon}\rho\,\mathbf{v}\,\mathrm{d}\upsilon = \int_{\partial\upsilon}\rho\,\mathbf{v}\,v_n\,\mathrm{d}s = \int_{\partial\upsilon}\boldsymbol{\tau}\cdot\mathbf{n}\,\mathrm{d}s + \int_{\mathrm{d}\upsilon}\rho\,\mathbf{g}\,\mathrm{d}\upsilon\,, \tag{2}$$

$$\frac{\mathrm{D}(e+k)}{\mathrm{D}t} = \frac{\partial}{\partial t}\int_{\mathrm{d}\upsilon}\left(e+\frac{v^2}{2}\right)\rho\,\mathrm{d}\upsilon + \int_{\partial\upsilon}\rho\left(e+\frac{v^2}{2}\right)v_n\,\mathrm{d}s = -\int_{\partial\upsilon}p\,\mathbf{n}\cdot\mathbf{v}\,\mathrm{d}s + \int_{\partial\upsilon}q\,\mathrm{d}s + \int_{\mathrm{d}\upsilon}\mathbf{g}\cdot\mathbf{v}\rho\,\mathrm{d}\upsilon\,. \tag{3}$$

Here e is the total thermal energy, including the chemical e_0 (6), k the kinetic energy, both intensive, ρ is the density and γ the adiabatic exponent of the working fluid, while υ is the control volume. The index n and vector $\mathbf{n}$ designate the external normal to any control volume. With no mass transfer along the channel, heat addition by a constant flux q is considered in the equation of energy, while friction τ is considered within the conservation law for the impulse (5), with gravitation of constant intensity $\mathbf{g}$. A cylindrical circular channel of radius R_i was further assumed in (5) with the loss of energy by friction fully recovered into heat, rendering

$$\begin{cases} \dfrac{\partial\rho}{\partial t} + \dfrac{\partial(\rho v)}{\partial x} = 0, \\ \dfrac{\mathrm{d}v}{\mathrm{d}t} + \dfrac{1}{\rho}\dfrac{\partial p}{\partial x} = -\dfrac{\tau}{\rho}\dfrac{2}{R_i} - g, \\ \dfrac{\mathrm{d}e}{\mathrm{d}t} + \dfrac{p}{\rho}\dfrac{\partial v}{\partial x} = \dfrac{q}{\rho}\dfrac{2}{R_i} - gv. \end{cases} \tag{5}$$

This hyperbolic system apparently involves four dependent variables ρ, p, T and v. It is not the case, however, because the equation of state is considered that reduces the number of self-dependent variables to three. The thermal energy of the gas mixture does not enter as an extra variable also, because it keeps proportional to the absolute temperature,

$$e = e_0 + c_V T\,. \tag{6}$$

The constant e_0 is the relative chemical energy for reacting mixtures. However, for the sake of simplicity, we shall further ignore the chemical behavior. The numerical scheme *TRANSIT* is now based on the vector $(p,\, v,\, \ln T)^{\mathrm{T}}$ of dependent variables. To structure this vector the density is replaced by $\rho = p/(RT)$ and its derivative $d\rho$ by its counterpart

$$\mathrm{d}\rho = \frac{\mathrm{d}p}{RT} - \frac{p}{RT}\mathrm{d}\ln T\,. \tag{7}$$

This is only to show that the given system of PDE-s presents the hyperbolic matrix form [12], [13], [14], [15],

$$[a]\frac{\partial(u)}{\partial t}+[b]\frac{\partial(u)}{\partial x}=(c)\,, \tag{8}$$

where the final vector of the unknown variables is $(u)^{\mathrm{T}}=[p, v, \ln T]$. The square 3×3 core matrices $[a]$ and $[b]$ are common for any ideal gas motion and are given by

$$[a]=\begin{bmatrix}1 & 0 & -p\\ 0 & 1 & 0\\ 0 & 0 & 1\end{bmatrix}, \qquad [b]=\begin{bmatrix}v & p & -vp\\ \dfrac{RT}{p} & v & 0\\ 0 & \gamma-1 & v\end{bmatrix} \tag{9}$$

while the free term vectors are

$$(c)_{MGT}=\begin{pmatrix}0\\ -\dfrac{2}{R_i}\dfrac{\tau}{\rho}-g\\ (\gamma-1)\left[\dfrac{q}{p}\dfrac{2}{R_i}-\dfrac{gv}{RT}\right]\end{pmatrix}. \tag{11}$$

By spectral resolution the given system of PDE-s is now transformed into an ODE system along the eigen characteristic directions in the *x-t* space, after the left eigen vectors e^{T} [12] are found. This always proves possible because the determinant of the main matrix $[a]$ is positively defined [3]. The system (8) will be re-cast [12] in the form:

$$(e)_j^T\frac{d_j(u)}{dt}=(e)_j^T(g) \quad \Big|\, j=1,2,3 \tag{14}$$

where the transformed free term vector **g** is given by

$$(g)\equiv[a]^{-1}\cdot(c)\,. \tag{15}$$

Note first that the inverse of **A** and the recurring matrix simply are

$$[a]^{-1}=\begin{bmatrix}1 & 0 & p\\ 0 & 1 & 0\\ 0 & 0 & 1\end{bmatrix}, \qquad [f]=\begin{bmatrix}v & \rho a^2 & 0\\ \dfrac{1}{\rho} & v & 0\\ 0 & \gamma-1 & v\end{bmatrix}.$$

The spectrum λ_j of the eigen matrix $[f]$ as the roots of the equation $\left|[f]-\lambda\,[\mathrm{E}]\right|=0$,

$$\begin{vmatrix}v-\lambda & \rho a^2 & 0\\ \dfrac{1}{\rho} & v-\lambda & 0\\ 0 & \gamma-1 & v-\lambda\end{vmatrix}=(v-\lambda)\left[(v-\lambda)^2-a^2\right]=0 \tag{16}$$

where the isentropic speed of sound a, $a^2\equiv\gamma RT$, helps define, based on the eigen values $\lambda_1=v+a$, $\lambda_2=v-a$, $\lambda_3=v$, the three characteristic directions in the *x-t* space.

Note that the spectrum of eigen values and the associated directions are identical with those for any other motion involving any ideal gases. The manner into which the wave front develops is specific however, due to the particular characteristic equations. The three left-eigen vectors accompanying these roots result now from the three corresponding equations

$$(e_j)^{\mathrm{T}}\left([f]-\lambda_j[E]\right)=(0)^{\mathrm{T}} \qquad \left|\, j=1,2,3\right. \tag{21}$$

With the assumption for a given, arbitrary constant equal to one, these eigen-vectors defining the right "+", the left "-" characteristics and the streamline "0" are

$$(e_+)=\begin{pmatrix}1\\ \rho a\\ 0\end{pmatrix},\qquad (e_-)=\begin{pmatrix}1\\ -\rho a\\ 0\end{pmatrix},\qquad (e_0)=\begin{pmatrix}1\\ 0\\ -\dfrac{\rho a^2}{\gamma-1}\end{pmatrix}. \tag{23}$$

Here (e_0) should not be confused with the scalar chemical energy in (6). Up to this point the non-isentropic problems are common. The distinct part of the method only comes into action when the characteristic equations are approached, where the different free terms play a role. The vector of the free terms results from equation (15) into the form (24) when the notations are used,

$$r\equiv\frac{\rho}{\rho_p},\qquad \theta\equiv\frac{T}{T_a},\qquad (g)_{MGT}\equiv\begin{pmatrix}(\gamma-1)\dfrac{4}{D}q\\ -g-\dfrac{2}{R_i}\dfrac{\tau}{\rho}\\ (\gamma-1)\left[\dfrac{2}{R_i}\dfrac{q}{p}-\dfrac{gv}{RT}\right]\end{pmatrix}, \tag{24}$$

while the very characteristic equations (14) for MGT become

$$\begin{cases}\dfrac{\mathrm{d}_+p}{\mathrm{d}t}+\rho a\dfrac{\mathrm{d}_+v}{\mathrm{d}t}=(\gamma-1)q\dfrac{2}{R_i}-\rho a\left(g+\dfrac{2}{R_i}\dfrac{\tau}{\rho}\right),\\ \dfrac{\mathrm{d}_-p}{\mathrm{d}t}-\rho a\dfrac{\mathrm{d}_-v}{\mathrm{d}t}=(\gamma-1)q\dfrac{2}{R_i}+\rho a\left(g+\dfrac{2}{R_i}\dfrac{\tau}{\rho}\right),\\ \dfrac{\mathrm{d}_0p}{\mathrm{d}t}-\dfrac{\gamma}{\gamma-1}p\dfrac{\mathrm{d}_0\ln T}{\mathrm{d}t}=-q\dfrac{2}{R_i}+\gamma\rho gv.\end{cases} \tag{27}$$

The finite differences are based on the grid built on the local wave front, where the positions for the upcoming node and of the streamline source result successively from equations (28). The computational nodes within each characteristic tetragon are denoted through A, E, C and D from left to right in the increasing sense of the space coordinate.

Passing now to finite differences to obtain all required equations in the working form for the solar receiver and the tower zones, with gravitation, heat exchange and drag, the working form of the system (27) becomes

$$\begin{cases} v_D - v_A + \dfrac{1}{(\rho a_S)_m}(p_D - p_A) = G_+(m)(t_D - t_A), \\ v_D - v_C + \dfrac{1}{(\rho a_S)_m}(p_D - p_C) = G_-(m)(t_D - t_C), \\ T_D - T_B = \dfrac{\gamma - 1}{\gamma}\dfrac{1}{\rho_B R}\left[p_D - p_B + \left(\dfrac{2}{R_i} q - \gamma \rho_B g v_B \right)(t_D - t_B) \right], \end{cases} \tag{29}$$

where m denotes the mean values between nodes A and C within the current wave front. In contrast to the situation in (28), here the mediation of the values for the speed of sound and the density between A and C within the left and right characteristics proved highly profitable for the regularity of the computational mesh [7]. Based on the same observation, the functions G_+ and G_- for the receiver (*rec*) and tower (*tow*) zones are,

$$G_+^{rec}(\rho, a) = \frac{2}{R_i}\frac{1}{(\rho a)_m}[(\gamma - 1) q - a_m \tau] , \qquad G_+^{tow} = -g ,$$

$$G_-^{rec}(\rho, a) = \frac{2}{R_i}\frac{1}{(\rho a)_m}[-(\gamma - 1) q - a_m \tau] , \qquad G_-^{tow} = -g . \tag{30}$$

From equations (29) the values for all the parameters of the flow in every new node D result, as a first order, linearized output,

$$\begin{cases} v_D = \dfrac{v_A + v_C}{2} + \dfrac{p_A - p_C}{(\rho a)_A + (\rho a)_C} + g_+(m), \\ p_D = \dfrac{p_A + p_C}{2} + \dfrac{(\rho a)_A + (\rho a)_C}{2}\left[\dfrac{v_A - v_C}{2} + g_-(m) \right], \\ T_D = T_B + g_0^{rec}(t_D - t_B). \end{cases} \tag{31}$$

where the notations $g_+^{rec} = G_+^{rec} \cdot (t_D - t_A)/2$ and $g_-^{rec} = G_-^{rec} \cdot (t_D - t_C)/2$ were used.

4. RESULTS FOR MIRROR GRAVITATIONAL TOWERS

A constant heat flux of 10 kW/m^2 was considered, as described at the end of chapter 1, for the heater part with the length of 3 meters of a constant area cylindrical tower with the overall diameter of 2 meters and a total height of 200 meters. Within the heater a *Hagen-Poiseuille* type friction loss $\tau = k \dfrac{4}{R_i} \rho \nu v_m$ of 5 *Pa* was also considered at 10 *m/s* mean air velocity. With an air viscosity ν=1·10-^{5} m^2/s and ρ=1.25 kg/m^3 this results in k=10^4. A regular grid with an initial step of 1*m* was applied along the tower, ending in 201 initial nodes where the initial velocity is zero, v_0=0. Initially the temperature-pressure distribution into the tower and around are the same, but beginning from t=0 the heat flux acts and produces a small compression wave that travels along the right characteristic up through the tower.

The flow is fully unsteady and steep variations in temperature and speed manifest, as given in figures 6-7 for two stations within the heater and for the exit area from above.

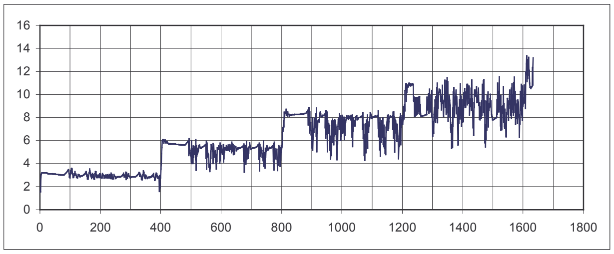

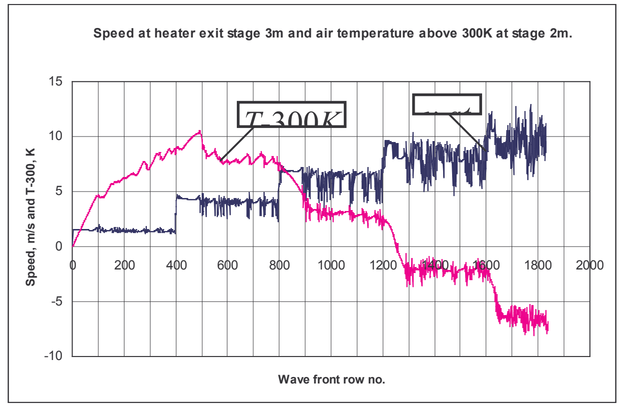

Figure 6: Air speed at exit, at heater end and temperature above 300K.

Due to the fast heating and subsequent dilatation of the air within the first 3 meters where the heater is located, the air expands on both sides up and down and thus a small reversed flow towards below the tower appears at the entrance. Thereafter a stepwise increment in the airspeed appears, while the cause itself, namely the heating and the temperature raise within the heating zone preserve continuous (Fig. 6). The evolution of the temperature itself goes through a maximum during the first 2 seconds and thereafter lowers below the ambient temperature for the rest of the time. The demonstration of the code was applied for the first 6 seconds of the tower transient, with steady state not been fully achieved. The first wavy motion along the tower lasts about 0.566 second, after which the first air motion is felt at the upper exit. At that moment an expansion wake is reflecting below which arrives at the entrance after 0.57 more seconds producing the first air admission into the tower. The stepwise velocity increment is perhaps a consequence of the long time constant of the air within the tower and does not derive from numerical effects.

5 CONCLUSIONS

The one-dimensional method of characteristics appears as an efficient and accurate tool for the simulation of the purely gasdynamic transient work of rocket engines with high length-to-diameter ratios, if the method is augmented with thickening and leveling of the computational mesh. Nevertheless, it was clearly observed that a double density mesh has a small effect on the results, the method being stable and efficient. Repeated tests of the code revealed that the thickening of the mesh nodes through Spline interpolation (Micula 1978) or Bezier interpolation (Mortari 2007) is very smooth and substantially contributes to the stability of the scheme. A major improvement was also introduced when the adjacent characteristic lines are merged into small shock that is carried along the very characteristics downwind. The TRANSIT code is much aggressed, due to the very small variations in flow parameters values that scatter each other with increasing effects. Even the faintest bumps in the velocity or the speed of sound produce small shocks followed by a rarefaction of the characteristic lines. Behind this shocks a fan is accumulating that gradually develops into irregularities of the computational mesh. The acceptance of locally reversed flows also plays a main role in providing a reliable code for the MGT case. It seems that the computational task involving the draught towers is a barrier type proof of the unsteady method and the numerical code. Further improvements are also envisaged for a multidimensional analyzes.

REFERENCES

[1] Zannetti, L., Favini, B., “Wave Propagation Phenomena as Tools for the Study of Inviscid Compressible Flows”, *Proc. High Speed Aerodynamics II Symposium, ed. A. Nastase, Aachen, Germany,* 1990, pp. 155-169.

[2] Rugescu, R. D., “Modeling of one-dimensional unsteady flows in rocket engines”, *Revue Roumaine des Sciences Techniques-Mecanique Appliquee*, **46**, 1-6(2001), pp. 97-109.

[3] Rugescu, R. D., Avasilichioaiei, D., “A Method of Characteristics Approach for Nonisentropic Transients in Rocket Engines”, *Scientific Bulletin of the University ”Politehnica” of Bucharest*, series D, Mechanical Engineering, **61**, 3-4(1999), pp. 311-324.

[4] Rugescu R. D., *Thermische Turbomaschinen*, ISBN 973-30-1846-5, Ed. D. P. Bucharest, Ch.7, 2005.

[5] Rugescu, R. D., Chiciudean, T. G., Toma, A. C., Tache, F., “Thermal Draught Driver Concept and Theory as a Tool for Advanced Infra-Turbulence Aerodynamics”, in *DAAAM International Scientific Book 2005*, ISBN 3-901509-43-7, B. Katalinic (Ed.), Viena, pp. 543-557.

[6] Tache, F., Rugescu, R. D., Slavu, B., Chiciudean, T. G., Toma, A. C., Galan, V. “Experimental Demonstrator of the Draught Driver for Infra-Turbulence Aerodynamics”, *Annals of DAAAM for 2006 & Proceedings of the 17th International DAAAM Symposium*, ISSN 1726-9679 ISBN 3-901509-57-7, Editor B. Katalinic, Published by DAAAM International, Vienna, Austria 2006, pp. 409-410.

[7] R.D. Rugescu, “Technology of CFD in space engines and solar-gravitational power plants”, *International Journal of Energy Technology and Policy*, ISSN 1472-8923, On-line ISSN 1741-508X, 2007 (in press).

[8] Haaf, W., “Solar Chimneys, Part II: Preliminary Test Results from the Manzanares Pilot Plant,” Int. J. Sol. Energy, **2** (1984), pp. 141–161.

[9] Pretorius J. P., Solar Chimney Power Plant Performance, *ASME Journal of Solar Energy Engineering*, ISSN 0199-6231, Aug. 2006, Vol. 128 Issue 3, pp. 302-311.

[10] Feidt, M., Costea, M., Petre, C., Boussehain, R., *Génie Energétique Appliqué au solaire; Energie Solaire Thermique*, Editura Printech, 2004, ISBN 973-718-092-5 (115 pages en français).

[11] Rugescu, R. D., Tache, F., Chiciudean, T. G., Toma, A. C., Slavu, B., Galan, V. “Project SEATTLER for Renewable Electricity”, Chapter 42 in *DAAAM International Scientific Book 2006*, B. Katalinic (Ed.), DAAAM International, ISBN: 3-901509-43-7, ISSN 1726-9687, Viena, Austria, 2006, pp. 523-538.

[12] Ballmann, J., “Introduction to Gasdynamics”, *Space Course Aachen*, Aachen, 1991.

[13] Evans, L.C., *Partial Differential Equations*, American Mathematical Soc., Providence 1998 ISBN 0-8218-0772-2.

[14] Thomas, J., *Numerical Partial Differential Equations: Conservation Laws and Elliptic Equations*, Springer, 1999.

[15] Polyanin, A. D., Zaitsev, V. F. and Moussiaux, A., *Handbook of First Order Partial Differential Equations*, Taylor & Francis, London, 2002. ISBN 0-415-27267-X.

[16] Micula N., Functii Spline si aplicatii, Ed. Tehnica, Bucuresti 1978.

[17] Mortari D., Rugescu R. D., Karimo, J. (2007), “Bezier Representation of Analytical Functions and Applications”, to be submitted to *Journal of Approximation Theory*.

[18] Gannon, A. J., Von Backström, T. W., Solar Chimney Turbine Performance, *ASME Journal of Solar Energy Engineering*, **125**, 2003, p101-106.

[19] Schlaich J., Bergermann R., Schiel W., Weinrebe G. (2004), Design of Commercial Solar Updraft Tower Systems – Utilization of Solar Induced Convective Flows for Power Generation, *Commercial Solar Towers JSEE Rev.C2*.

[20] Unger, J., *Konvektionsströmungen*, B. G. Teubner, ISBN 3-519-03033-0, Stuttgart, 1988.

[21] Weinrebe G. (2004), Das Aufwindkraftwerk-Wasserkraftwerk der Wüste, *Nova Acta Leopoldina* NF91, Nr.339, pp. 117-141.